demonstrated TGF-β1 can act as a tumor suppressor or a tumor promoter depending on the characteristics of the cell.

There is increasing evidence that loss of the growth-inhibitory effects of TGF-β1 appears to be an important event for malignant transformation of epithelial cells.[2] Sheng et al[2] have demonstrated that chronic TGF-β1 treatment leads to malignant transformation through downregulation of TGF-β type II receptor and induction of cyclooxygenase-2 in rat intestinal epithelial cells.[2] A recent study[3] has demonstrated that TGF-β1 expression is markedly enhanced in the ductal epithelial and stromal cells of invasive ductal pancreatic adenocarcinomas (DPAs), although the precise role of TGF-β1 in the progression of pancreatic cancer remains unclear.

We hypothesized that TGF-β1 might induce malignant transformation of pancreatic epithelial cells during the development of pancreatic cancer. In the present study, we examined TGF-β1 expression in pancreatic intraepithelial neoplasias (PanINs), which have been thought to be precancerous lesions of invasive DPAs, and whether TGF-β1 exposure could confer the malignant phenotype in conditionally immortalized pancreatic epithelial (IMPE) cells established from a temperature-sensitive SV40 Large T antigen (SV40 LT Ag) transgenic mouse.[4]

MATERIAL AND METHODS

Antibodies. Rabbit anti—TGF-β1 (clone V) and anti-TGFβIIR (clone L-21), goat anti-$p15^{INK4b}$ (clone M-20), and mouse anti-smad4 (clone B-8), anti-p16INK4a (clone M-156), anti-$p21^{WAF1/CIP1}$ (clone C-19), anti-CDK2 (cloneM2), anti-cyclin A (clone C-19), anti-cyclin B1 (clone GNS), anti-cyclin D1 (clone R-124), and anti-cyclin E (clone M-20) were purchased from Santa Cruz Biotechnology (Santa Cruz, Calif). Mouse anti-cdc2 (cat. no. C12720) and anti-$p27^{KIP1}$ (cat. no. K25020) were obtained from BD Transduction Laboratory (San Jose, Calif). Mouse anti—β-actin (cat. no. A-5441) was purchased from Sigma Chemical Co (St. Louis, Mo). Mouse anti-SV40 LT Ag was obtained from Oncogene (Darmstadt, Germany). Rabbit anti-p53 (cat. no. 9282) and anti—phospho-smad2 (cat. no. 3101) were purchased from Cell Signaling Technology (Beverly, Mass).

Tissue samples. Formalin-fixed, paraffin-embedded tissues were collected from the Department of Surgery and Surgical Basic Science, Kyoto University, between January 1994 and December 2000. Tissue specimens were collected from patients who provided informed consent, in accordance with institutional guidelines. These specimens were from 22 patients with invasive DPA. Among the specimens, 61 lesions were examined by hematoxylin and eosin staining for the classification of PanINs in this study. The classification was performed by 2 pathologist experts in pancreatic pathology.

Immunohistochemical analysis. Serial, 4-μm-thick sections were deparaffinized in 3 changes of xylene, rehydrated in descending concentrations of ethanol, and washed 3 times for 5 minutes each with double-d—distilled water. After rehydration, the sections were placed in 0.01 mol/L sodium citrate buffer (pH 6.0) for 20 minutes at 95°C and then incubated for 30 minutes at room temperature (RT) in 0.3% hydrogen peroxide in methanol to block endogenous peroxidase activity. The sections were then incubated for 30 minutes at RT with 0.01 mol/L phosphate-buffered saline (PBS) (pH 7.4) that contained 1% normal goat serum and 1% bovine serum albumin (fraction V; Sigma) followed by overnight incubation at 4°C with a primary antibody, which was diluted 1:100 in 0.01 mol/L PBS that contained 1% normal goat serum and 1% bovine serum albumin. The sections were washed 3 times for 5 minutes in PBS and incubated for 60 minutes with horseradish peroxidase—conjugated antirabbit immunoglobulin G (Envision Kit; DakoCytomation, Kyoto, Japan) as a secondary antibody. The serial sections were stained with hematoxylin and eosin, and the sections with confirmed diagnosis of PanINs were subjected to TGF-β1 expression analysis. The specimens with TGF-β1—positive cells of more than 25% of the total cell number among PanIN lesions were regarded as positive, and those with positive cells of less than 25% were regarded as negative. The evaluation of immunostaining was performed by 2 investigators (D.I. and K.F.).

Cell culture and treatment with TGF-β1. Conditionally immortalized pancreatic epithelial (IMPE) cells were used in this study.[4] This cell line was established from the pancreas of a temperature-sensitive SV40 LT Ag transgenic mouse. The cells were grown in RPMI 1640 (Gibco-BRL, Grand Island, NY) supplemented with 5% fetal bovine serum (FBS) (Gibco-BRL), antibiotics, 10 U/mL of murine interferon-γ (IFNγ) (cat. no. IM-112A; Gibco-BRL) and 20 ng/mL of bovine insulin (cat. no. 13007-018; Gibco-BRL), and maintained in a 5% humidified CO_2 atmosphere at 33°C. IMPE cells have the characteristics of epithelial cells, mainly duct cells, since they express E-cadherin, β-catenin, and cytokeratin 8 and 18 as well as cytokeratin 19. The cells proliferate continuously

at the permissive condition (33°C with IFNγ), but proliferation ceases at the nonpermissive condition (39°C without IFNγ).[4] Therefore, IMPE cells may behave as normal pancreatic epithelial cells when they are cultured at the nonpermissive condition and might be a useful model for the study of processes involved in pancreatic carcinogenesis.

To analyze the effects of TGF-β1 on IMPE cells, we incubated cells with various concentrations of recombinant human TGF-β1 (cat. no. 240-B, R&D systems; Minneapolis, Minn) after 24-hour serum starvation. For long-term exposure to TGF-β1 (≥50 days), complete medium containing 1 ng/mL of TGF-β1 was replaced every 3 days.

Cell proliferation assay. IMPE cells (1×10^4) were placed in 24-well tissue culture dishes at 33°C. The number of cells was counted at the indicated time by a cell counter (Coulter Z1; Beckman-Coulter, Fullerton, Calif). For cell growth at the nonpermissive condition, cells were incubated at 33°C overnight, and subsequently the medium was changed to IFNγ-free medium followed by incubation at 39°C for the indicated time.

Anchorage-independent growth. For soft agar assay, 5×10^4 cells were suspended in 1 mL of 0.8% agarose (Difco, Detroit, Mich) in RPMI supplemented with 10% FBS and placed on 6-well plate dishes coated with 1 mL of 1% agar (Difco) in RPMI with 10% FBS. For Matrigel assay, 2×10^4 cells were suspended in 2 mL of 1:2 diluted Matrigel (BD Biosciences, Bedford, Mass). The mixture was plated on 6-well plate dishes. A 1-mL complete medium was added to cover the Matrigel. Cultures were incubated at 33°C; colony formation was observed after 2 weeks by phase-contrast microscopy.

Western blot analysis. Cells were lysed in RIPA buffer containing 50 mmol/L HEPES (pH 7.0), 250 mmol/L NaCl, 0.1% Nonidet P-40, 1 mmol/L phenylmethylsulfonylfluoride, and 20 μg/mL gabexate mesilate, and incubated on ice for 10 minutes. The lysate was then sonicated for 10 seconds. Total extracts were cleaned by centrifugation at 15,000 rpm for 10 minutes at 4°C, and the supernatants were collected. Protein concentration was measured by a protein assay reagent (cat. no. 23223, 23224; Pierce, Rockford, Ill). The lysates were resuspended in 1 volume of the gel-loading buffer, which contained 50 mmol/L Tris-HCl (pH 6.7), 4% SDS, 0.02% bromophenol blue, 20% glycerol and 4% 2-mercaptoethanol, and then heated at 95°C for 5 minutes. The extracted protein was subjected to Western blotting as previously described. In brief, 30-μg aliquots of protein were size fractionated to a single dimension by SDS-PAGE (8%-15% gels) and transblotted to a 0.45-μm polyvinylidine difluoride membrane (IPVH304F0; Millipore, Billerica, Mass) in a semidry electroblot apparatus (Bio-Rad, Richmond, Calif). The blots were then washed 3 times in Tris-buffered saline with 0.1% Tween-20 (TBST) and incubated for 1 hour at RT in blocking buffer (Block Ace; Dainipponseiyaku, Osaka, Japan). Subsequently, the blots were immunoblotted with an appropriate primary antibody for 1 hour at RT or overnight at 4°C. Unbound antibody was removed by washing the membrane with TBST 3 times, each for 10 minutes. The membrane was then incubated with a horseradish peroxidase–conjugated secondary antibody for 1 hour at RT followed by the addition of TBST as described above. Antibody reaction was detected by the enhanced chemiluminescence system (Amersham, Buckinghamshire, United Kingdom). The membranes were treated with enhanced chemiluminescence reagents according to the manufacturer's protocol and were exposed to x-ray films for 5 to 120 seconds.

Reverse-transcriptase polymerase chain reaction. Total cellular RNA was prepared with the use of TRIZOL Reagent (Life Technologies, Rockville, Md); complementary DNA (cDNA) was prepared by random priming from 1 μg of total RNA with the use of a First-Strand cDNA Synthesis kit (Pharmacia Biotech, North Peapack, NJ) according to the manufacturer's instructions. The reverse-transcriptase polymerase chain reaction (RT-PCR) analysis was performed as previously described.[5] The sequences for the primers used in this study are as follows:

β-actin: (sense) atggatgacgatatcgct, (antisense) atgaggtagtctgtcaggt

TGF-β type II receptor: (sense) acgtgagactgtccacttg, (antisense) atgacacacttgggagaag

Smad2: (sense) gatgactacacccactccattccag, (antisense) ctcagcaaacacttccccacctatg

Smad3: (sense) ctggctacctgagtgaagatggaga, (antisense) aaagacctcccctccgatgtagtag

Smad4: (sense) gtctaatgccaccagtaccaccaac, (antisense) tgacccaagcaaaagcgatctcctc

Smad7: (sense) aatggcttttgcctcggacagc, (antisense) cacaaagctgatctgcacggtg

The products were 569 (β-actin), 205 (TGF-β type II receptor), 465 (smad2), 368 (smad3), 485 (smad4), and 321 (smad7) base pairs.

Tumorigenicity assay. IMPE or IMPE-Tr cells suspended in 100 μl of PBS (2×10^6) were injected into the dorsal subcutaneous tissue of nude mice (Balb/c, nu/nu). After tumors developed to the size of 1 × 1 cm, the mice were sacrificed. Tumor tissues were fixed, stained with hematoxylin

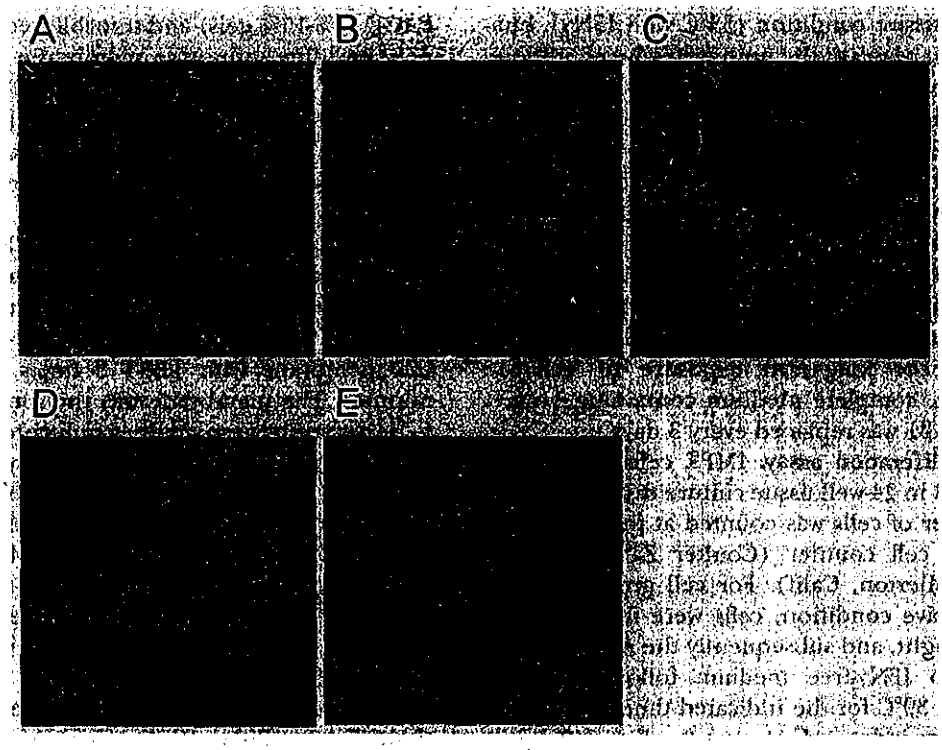

Fig 1. Immunohistochemical analysis of TGF-β1 expression in normal pancreatic ducts and PanIN lesions. **A,** No staining was detected in normal ducts. Typical photomicrographs of PanIN lesions regarded as positive are shown: **B,** PanIN-1a; **C,** PanIN-1b; **D,** PanIN-2; **E,** PanIN-3. Membranous and cytosolic staining of TGF-β1 was seen in these sections. The nuclei were counterstained with Mayer's hematoxylin (Original magnification ×400).

and eosin, and processed for histopathologic analysis.

Statistical analysis. Results are presented as mean ± SEM. Data were analyzed by the Student *t* test; statistical significance was considered to be present at a *P* value of less than .05. Each experiment was repeated independently at least 3 times.

RESULTS

TGF-β1 expression in PanINs. To examine the involvement of TGF-β1 during pancreatic carcinogenesis, we performed immunohistochemical analysis of PanINs. Similar to the adenoma–carcinoma sequence of colon cancer, PanINs are thought to be precancerous lesions of pancreatic cancer that include flat lesions without atypia (PanIN-1a), papillary lesions without atypia (PanIN-1b), papillary lesions with atypia (PanIN-2), and carcinoma in situ (PanIN-3).[6] Strong membranous and cytosolic staining of TGF-β1 was seen in 33.3% of PanIN-1a lesions, 52.2% of PanIN-1b lesions, 57.1% of PanIN-2 lesions, and 33.3% of PanIN-3 lesions, whereas no TGF-β1 staining in epithelia of normal pancreatic ducts was detected (Fig 1, Table).

Table. Proportions and percentage of TGF-β1 expression in PanIN lesions

	TGF-β1		
PanINs	*Negative (n = 33)*	*Positive (n = 28 [46%])*	*Total*
1a	6	3 (33.3%)	9
1b	11	12 (52.2%)	23
2	6	8 (57.1%)	14
3	10	5 (33.3%)	15
Normal ducts	5	0 (0%)	5

TGF-β1 inhibits proliferation of IMPE cells through upregulation of $p21^{WAF1/CIP1}$. We have established conditionally immortalized pancreatic epithelial (IMPE) cells from the pancreas of a transgenic mice harboring temperature-sensitive SV40 LT Ag, which binds and inactivates p53 and pRB proteins.[4] Using this cell line, we examined the growth-inhibitory effects of short-term exposure to TGF-β1 (0-12 days) on pancreatic epithelial cells. Exposure to 1 ng/mL of TGF-β1 inhibited the proliferation of IMPE cells by 75% at day 8 compared with that of untreated cells (Fig 2, *A*).

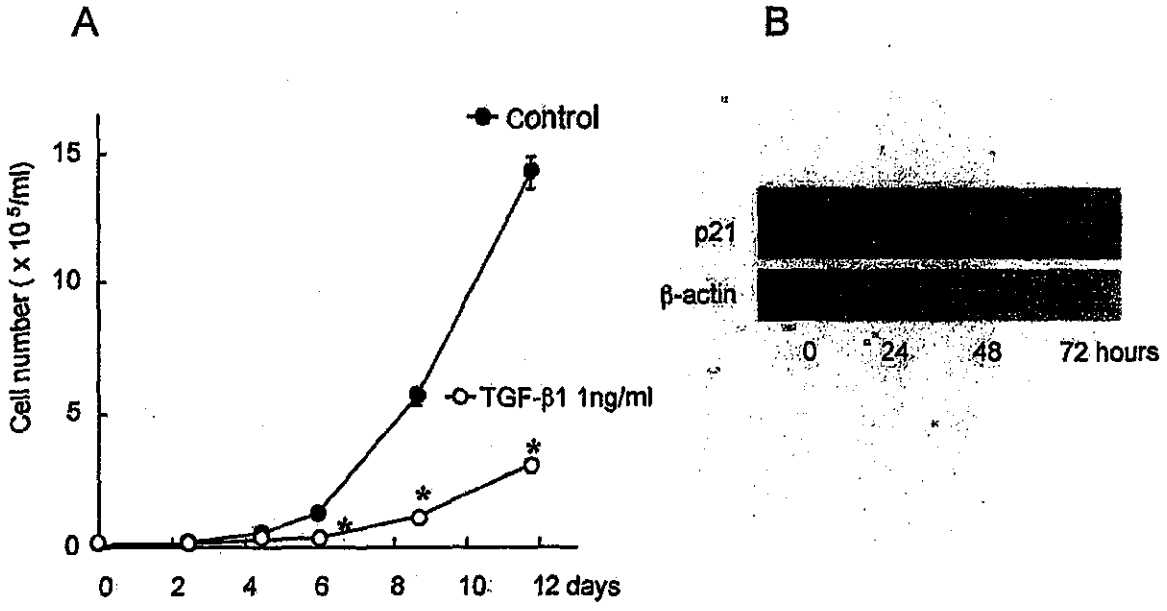

Fig 2. A, Growth-inhibitory effects by short-term exposure to TGF-β1. The proliferation of IMPE cells was inhibited by 75% at day 8 after the treatment of 1 ng/mL of TGF-β1. Data represent the mean ± SEM of triplicate inserts from 1 of 3 representative experiments. *Significant difference from the control group ($P < .05$). **B,** Induction of $p21^{WAF1/CIP1}$ by short-term exposure to TGF-β1. After 24-hour serum-starvation, IMPE cells were cultured with medium containing 5 ng/mL of TGF-β1 for 0, 24, 48, and 72 hours. $p21^{WAF1/CIP1}$ expression was examined by Western blot analysis. Its maximal expression was observed at 48 hours after the treatment.

Growth-inhibitory effects of TGF-β on epithelial cells have been reported to inhibit cell proliferation through regulation of cyclin-dependent kinase (CDK) inhibitors including $p15^{INK4B}$, $p21^{WAF1/CIP1}$, and $p27^{KIP1}$. Therefore, we next examined whether TGF-β1 treatment could alter the expression levels of CDK inhibitors in IMPE cells. Western blot analysis showed that exposure to 5 ng/mL TGF-β1 induced $p21^{WAF1/CIP1}$ protein in IMPE cells; the maximal expression was observed at 48 hours (Fig 2, *B*).

Establishment of TGF-β1 resistant IMPE (IMPE-Tr) cells by long-term TGF-β1 exposure. To determine whether long-term exposure to TGF-β1 could alter phenotypes of IMPE cells, the cells were cultured with a medium containing 1 ng/mL of TGF-β1 for more than 50 days. The TGF-β1–treated cells were referred to as IMPE-Tr cells. IMPE-Tr cells showed more spindle-shaped morphology compared with nontreated cells (Fig 3, *A*). With respect to the growth-inhibitory effects of TGF-β1, the proliferation of IMPE-Tr cells was inhibited by the treatment of 1 ng/mL of TGF-β1 by 45% at day 8, although that of parental IMPE cells was inhibited by 75% at day 8 (Fig 3, *B*). These data suggest that IMPE-Tr cells turned out to be partially resistant to the growth-inhibitory effects of TGF-β1.

Colony formation of IMPE-Tr cells in soft agar and Matrigel. Since long-term exposure to TGF-β1 rendered IMPE cells partially resistant to the growth-inhibitory effects of TGF-β1, we speculated that IMPE-Tr cells could acquire malignant phenotypes. The ability to form colonies in 3-dimensional culture is one of the characteristics of neoplastic transformation.[7] Therefore, we performed soft agar and Matrigel culture assays to examine the phenotypic alteration that occurred in IMPE-Tr cells. Colony formation was observed at day 14 with a low-power objective of an inverted microscope. Parental IMPE cells formed few colonies in soft agar and Matrigel, whereas IMPE-Tr cells formed many colonies in soft agar and Matrigel (Fig 4). The number of colonies cultured in Matrigel was 3.0 ± 1.6 for IMPE cells and 21.7 ± 6.8 for IMPE-Tr cells (mean ± SEM, $P < .05$).

Phenotypic alterations of IMPE-Tr cells are associated with downregulation of Smad2 phosphorylation and $p21^{WAF1/CIP1}$ induction by TGF-β1

We next investigated the mechanism involved in the acquisition of resistance to the growth-inhibitory effect of TGF-β1 in IMPE-Tr cells.

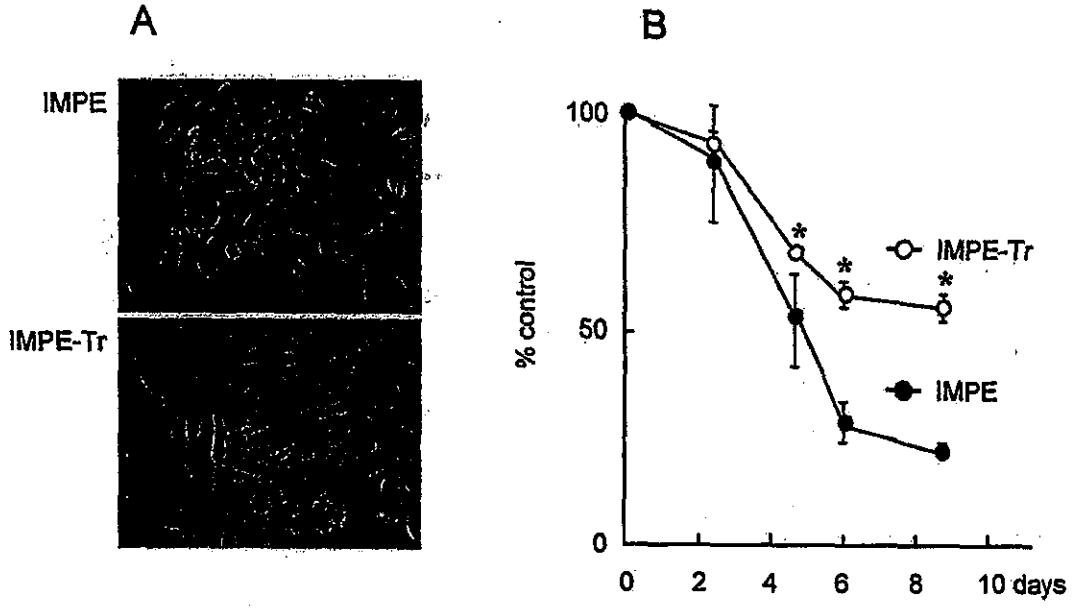

Fig 3. Establishment of IMPE-Tr cells. **A,** IMPE cells were cultured with medium containing 1 ng/mL of TGF-β1 continuously for more than 50 days. IMPE-Tr cells showed spindle-shaped morphology. **B,** Growth-inhibitory effects of TGF-β1 in IMPE-Tr cells were significantly reduced compared with that in parental IMPE cells. Data represent the mean ± SEM of triplicate inserts from 1 of 3 representative experiments. *Significant difference from the parental IMPE cells ($P < .05$).

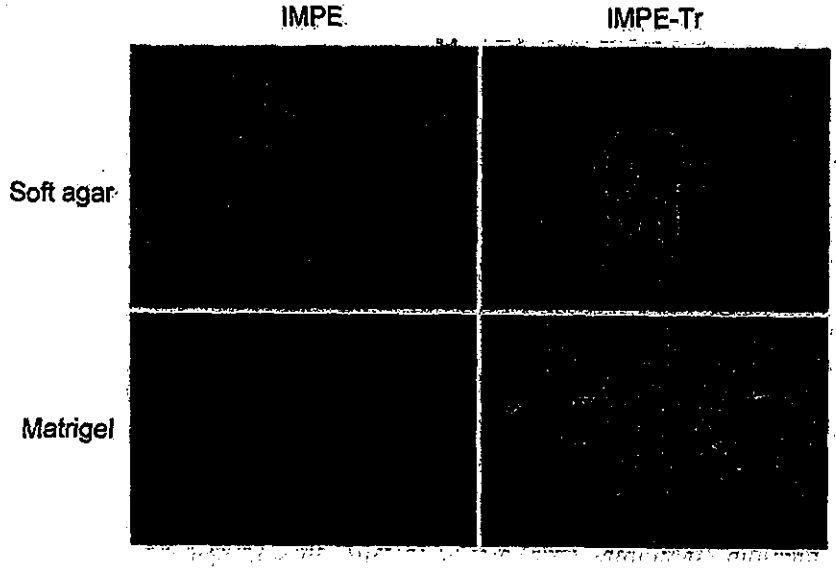

Fig 4. Anchorage-independent growth. IMPE and IMPE-Tr cells were cultured in soft agar (*upper panel*) and Matrigel (*lower panel*). Colony formation was observed at day 14. IMPE cells formed few clusters of cells in soft agar and Matrigel (*arrow heads*), whereas IMPE-Tr cells formed many colonies in soft agar and Matrigel (*arrows*).

Semiquantitative RT-PCR analysis revealed no difference in the expression of TGF-β type II receptor and smads (2, 3, 4, and 7) mRNA between IMPE cells and IMPE-Tr cells (Fig 5, *A*). Western blot analysis also showed no difference in the protein expression of TGF-β type II receptor and smad4 between both cells (data not shown). Phosphorylation of smad2 in IMPE and IMPE-Tr cells by treatment with 10 ng/mL of TGF-β1 was analyzed by Western blot analysis with the use of

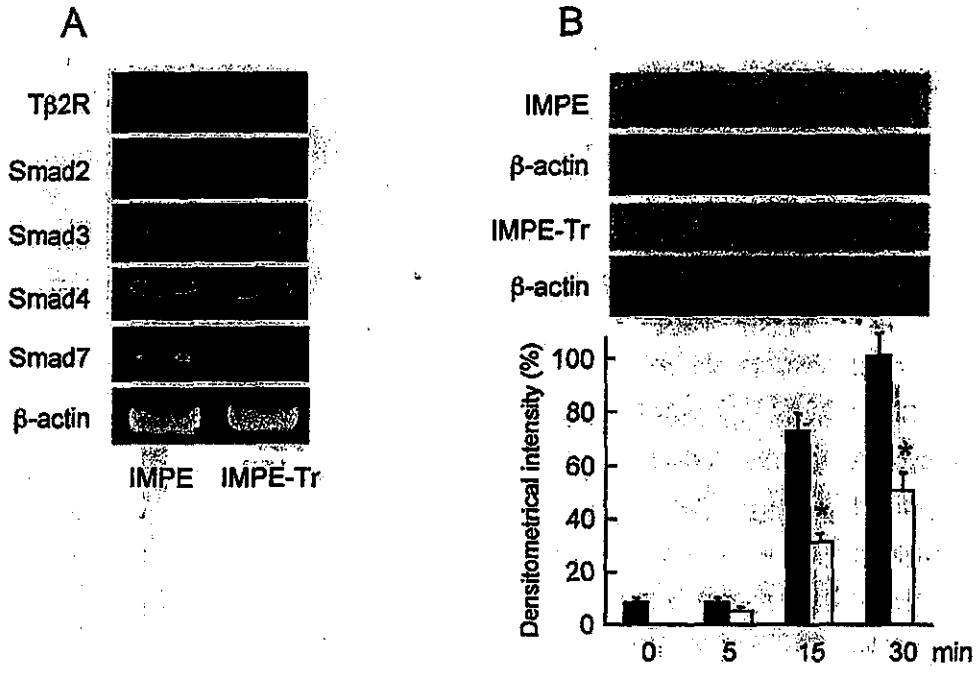

Fig 5. **A,** Semiquantitative RT-PCR of TGFβ type II receptor (TβIIR) and smads. **B,** Expression of phospho-smad2. Expression level of phosphorylation was evaluated by a densitometry (ATTO, Osaka, Japan). Although the increase of smad2 phosphorylation in both of IMPE and IMPE-Tr cells was found by 10 ng/mL of TGF-β1 treatment (*upper panel*), the phosphorylation was reduced by approximately 50% in IMPE-Tr cells compared with parental IMPE cells (*lower panel*). *Black* and *white bars* indicate the phosphorylation levels of IMPE and IMPE-Te cells, respectively. Data represent the mean ± SEM of triplicate inserts from 1 of 3 representative experiments. *Significant difference from the parental IMPE cells ($P < .05$).

a phospho-specific smad2 antibody. In both IMPE and IMPE-Tr cells, TGF-β1 treatment induced time-dependent phosphorylation of smad2. However, the timing of phosphorylation was delayed in IMPE-Tr cells, and the expression level of phosph-smad2 was weaker than that of parental IMPE cells (Fig 5, *B*).

Since TGF-β1 treatment induced $p21^{WAF1/CIP1}$ protein in IMPE cells and inhibited the proliferation, we also examined the expressions of cell cycle–associated proteins in IMPE and IMPE-Tr cells. All the CDK inhibitors, CDKs, and cyclins examined in this study were expressed at an equivalent level in nontreated IMPE and IMPE-Tr cells (Fig 6, *A*). On the other hand, the induction of $p21^{WAF1/CIP1}$ protein was significantly decreased by 8.3 % in IMPE-Tr cells 48 hours after the treatment of 5 ng/mL of TGF-β1 compared with that of parental IMPE cells (Fig 6, *B*).

Ability to form subcutaneous tumors in nude mice. Although parental IMPE cells did not proliferate indefinitely at 39°C, which is the body temperature of mice, IMPE-Tr cells did gain the ability to maintain indefinite growth after transient equilibrium even at 39°C (Fig 7, *A*). As shown in Fig 7, *B*, the IMPE-Tr cells that resumed proliferation showed no expression of $p21^{WAF1/CIP1}$ protein at day 15, although parental IMPE and IMPE-Tr cells at day 0 showed strong expression.

Finally, the ability to form subcutaneous tumors in nude mice was examined with the use of parental IMPE cells and IMPE-Tr cells, which acquired indefinite growth at 39°C. No tumor growth was observed in any of the mice injected with parental IMPE cells during 8 months of observation. In contrast, all 5 nude mice injected with IMPE-Tr cells developed subcutaneous tumors 12 weeks after the inoculation of the cells (Fig 7, *C*). Hematoxylin and eosin staining showed infiltration of the tumor cells into muscle tissue. Tumors were composed of cells with severe cellular atypia and mimicked poorly differentiated carcinoma.

DISCUSSION

This study demonstrates that the expression of TGF-β1 is seen even in PanIN lesions that have been thought to be precancerous lesions of pancreatic cancer, and that conditionally immortalized pancreatic epithelial cells might be conferred

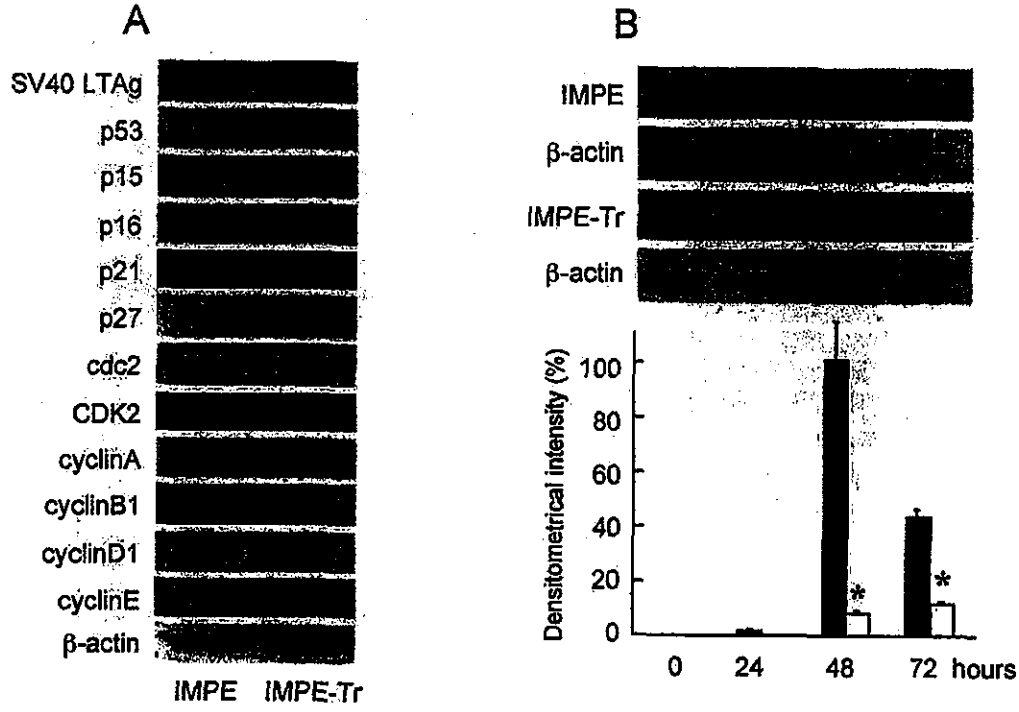

Fig 6. Western blot analysis of cell cycle–associated proteins. **A,** All of the proteins examined in this study expressed at an almost equivalent level in IMPE and IMPE-Tr cells after 24 hours of serum starvation. **B,** Expression of $p21^{WAF1/CIP1}$. Exposure to 5 ng/mL of TGF-β1–induced $p21^{WAF1/CIP1}$ and maximal expression was observed 48 hours after the treatment in IMPE-cells. In contrast, the expression of $p21^{WAF1/CIP1}$ induced by TGF-β1 treatment was markedly downregulated in IMPE-Tr cells. *Black* and *white bars* indicate $p21^{WAF1/CIP1}$ protein levels of IMPE and IMPE-Te cells, respectively. Data represent the mean ± SEM of triplicate inserts from 1 of 3 representative experiments. *Significant difference from the parental IMPE cells ($P < .05$).

the characteristics of malignant transformation by long-term exposure to TGF-β1. Furthermore, we have shown that the malignant transformation was associated with downregulation of smad2 phosphorylation and $p21^{WAF1/CIP1}$ induction.

We first demonstrated that TGF-β1 was expressed in PanINs but not in normal pancreatic ductal cells. Forty-six percent of PanIN lesions were positive for TGF-β1 expression; 54% were negative. We hypothesized that TGF-β1 expression might be related to the progression of pancreatic cancer. Although we expected that the proportion of lesions expressing TGF-β1 might increase along with progression of PanINs in this study, our data of TGF-β1 expression in PanINs (33.3% of PanIN-1a lesions, 52.2% of PanIN-1b lesions, 57.1% of PanIN-2 lesions, and 33.3% of PanIN-3 lesions) did not support the expectation (Table I). Recently, it has been reported that enhanced expression of TGF-β1 is observed in 47% of invasive DPAs.[3] Kazbay et al[8] showed that TGF-β1 was detected in 17 of 20 patients (85%) with chronic pancreatitis. Furthermore, Satoh et al[9] demonstrated there were no significant differences in the expression of TGF-β1 between pancreatic cancer and chronic pancreatitis. Although the reason why PanIN-3 lesions do not have a higher percentage than PanIN-2 lesions remains unclear, the fact that TGF-β expression was also found in chronic pancreatitis shows that TGF-β expression may not necessarily be associated only with the grade of malignancy. However, our data suggest that PanIN lesions could secrete TGF-β1 even in the early stage of PanINs and might be exposed to TGF-β1 in an autocrine manner.

It is very interesting to clarify the mechanism of TGF-β1 production in PanIN lesions. Since previous studies[10] have shown that an activating mutation of ras is detectable in early PanIN lesions and that transfection of ras or raf, a downstream effector of ras, induces TGF-β production in MDCK cells,[7,11] ras mutation might be related to enhanced TGF-β1 expression in PanINs. A study of the

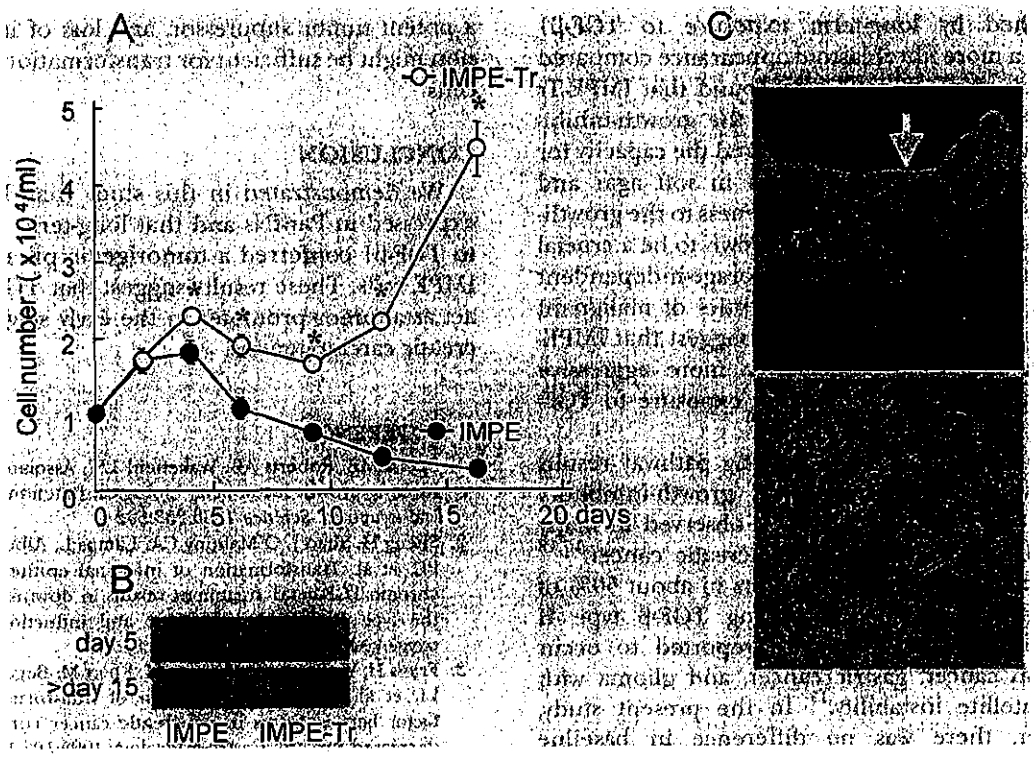

Fig 7. A, Proliferation assay at 39°C with medium containing 1 ng/mL of TGF-β1. IMPE cells did not proliferate at 39°C, but IMPE-Tr cells could proliferate indefinitely 2 weeks after being shifted to 39°C. Data represent the mean ± SEM of triplicate inserts from 1 of 3 representative experiments. *Significant difference from the parental IMPE cells ($P < .05$). **B,** Although strong $p21^{WAF1/CIP1}$ expression was observed at day 5 in both of IMPE and IMPE-Tr cells cultured at 39°C, the expression was not seen in IMPE-Tr cells cultured for more than 15 days with 1 ng/mL of TGF-β1 at 39°C. **C,** IMPE and IMPE-Tr cells were inoculated into dorsal subcutaneous tissues of nude mice. IMPE-Tr cells formed tumors in all of the treated mice, whereas IMPE cells formed no tumor. The arrow shows the tumor (size of 1 × 1cm) of a mouse treated by IMPE-Tr cells at 12 weeks after inoculation (*upper panel*). *Lower panel* is hematoxylin and eosin staining of the xenograft (original magnification ×400).

transfection of mutated ras gene using IMPE cells is currently ongoing in our laboratory to clarify the mechanism.

TGF-β1 is known to be a potent growth inhibitor of epithelial cells; its growth-inhibitory effect has been thought to be mediated, in part, through upregulation of cell cycle inhibitory proteins, such as $p15^{INK4B}$, $p21^{WAF1/CIP1}$, and $p27^{KIP1}$.[12] In addition, Datto et al[13] have reported that TGF-β1 can induce $p21^{WAF1/CIP1}$ through a p53-independent mechanism in HaCaT cells. In this study, we found that TGF-β1 treatment significantly inhibited the proliferation of IMPE cells with a marked increase of $p21^{WAF1/CIP1}$ in a time-dependent manner when cultured at 33°C. The maximal expression of $p21^{WAF1/CIP1}$ was observed 48 hours after the treatment. Since p53 is inactivated in IMPE cells by the expression of SV40 LT Ag at 33°C (Fig 6, *A*), the induction of $p21^{WAF1/CIP1}$ by TGF-β1 seems to be independent of the activation of p53.

There is increasing evidence that TGF-β1 may act as a tumor suppressor or a tumor promoter depending on the characteristics of the cell.[5,7,11,14,15] It has been reported that TGF-β1 suppresses the formation of carcinogen-induced benign skin tumors, but, once tumors develop, it enhances tumor progression to invasive spindle carcinomas in transgenic mice with keratinocyte-targeted expression of TGF-β1.[14] We have previously reported[13] that TGF-β1 induces epithelial–mesenchymal transition and promotes invasiveness in intestinal epithelial cells after transfection with activated Ras. Sheng et al[2] have also demonstrated that chronic TGF-β1 treatment leads to malignant transformation in rat intestinal epithelial cells, and observed downregulation of TGF-β type II receptor and induction of cyclooxygenase-2 in the transformed cells. From these studies, we examined the effects of long-term exposure to TGF-β1 on IMPE cells. IMPE-Tr cells

established by long-term exposure to TGF-β1 showed a more fibroblastoid appearance compared with parental IMPE cells. We found that IMPE-Tr cells were partially resistant to the growth-inhibitory effects of TGF-β1 and acquired the capacity for anchorage-independent growth in soft agar and Matrigel. Since loss of responsiveness to the growth-inhibitory effects of TGF-β is known to be a crucial step in carcinogenesis and anchorage-independent growth is one of the characteristics of malignant transformation,[16,17] our results suggest that IMPE-Tr cells might be conferred a more aggressive tumor phenotype by long-term exposure to TGF-β1.

Disruption of TGF-β–signaling pathway results in loss of responsiveness to growth-inhibitory effects of TGF-β and has been observed in many types of cancer, including pancreatic cancer.[17,18] Mutation of smad4/DPC4 occurs in about 50% of pancreatic cancer.[18] Inactivating TGF-β type II receptor mutation has been reported to occur in colon cancer, gastric cancer, and glioma with microsatellite instability.[17] In the present study, however, there was no difference in baseline expression of TGF-β type II receptor and smads, including smad4, between IMPE and IMPE-Tr cells. Intriguingly, we found that the phenotypic alterations of IMPE-Tr cells were accompanied by marked decrease in smad2 phosphorylation and $p21^{WAF1/CIP1}$ expression. Since smad2 has been reported to play a pivotal role in TGF-β–induced $p21^{WAF1/CIP1}$ expression,[17] downregulation of $p21^{WAF1/CIP1}$ was considered to be brought about by reduced smad2 phosphorylation. However, the detailed mechanisms by which long-term exposure to TGF-β1 accomplishes abrogation of smad2 phosphorylation in IMPE-Tr cells remain to be elucidated.

Finally, we examined the potential of tumorigenicity in nude mice since IMPE-Tr cells showed a more aggressive phenotype suggestive of neoplastic transformation in vitro at 33°C. Surprisingly, IMPE-Tr cells proliferated indefinitely at 39°C despite the lack of expression of SV40 LT Ag at this condition (data not shown). Western blot analysis revealed that $p21^{WAF1/CIP1}$ expression disappeared in IMPE-Tr cells after incubation for 2 weeks at 39°C. It seems that immortalization in IMPE-Tr cells at 39°C is not attributed to SV40 LT Ag expression but to the loss of $p21^{WAF1/CIP1}$ expression. Furthermore, we found that IMPE-Tr cells gained tumorigenic potential when injected subcutaneously into nude mice, while parental IMPE cells formed no tumor even 8 months after the inoculation. Thus, $p21^{WAF1/CIP1}$ may act as a potent tumor suppressor, and loss of its expression might be sufficient for transformation in IMPE cells.

CONCLUSION

We demonstrated in this study that TGF-β1 is expressed in PanINs and that long-term exposure to TGF-β1 conferred a tumorigenic phenotype in IMPE cells. These results suggest that TGF-β1 may act as a tumor promoter in the early stage of pancreatic carcinogenesis.

REFERENCES

1. Sporn MB, Roberts AB, Wakefield LM, Assoian RK. Transforming growth factor-beta: biological function and chemical structure. Science 1986;233:532-4.
2. Sheng H, Shao J, O'Mahony CA, Lamps L, Albo D, Isakson PC, et al. Transformation of intestinal epithelial cells by chronic TGF-beta1 treatment results in downregulation of the type II TGF-beta receptor and induction of cyclooxygenase-2. Oncogene 1999;18:855-67.
3. Friess H, Yamanaka Y, Buchler M, Ebert M, Beger HG, Gold LI, et al. Enhanced expression of transforming growth factor beta isoforms in pancreatic cancer correlates with decreased survival. Gastroenterology 1993;105:1846-56.
4. Koizumi M, Ito D, Fujimoto K, Toyoda E, Kami K, Mori T, Doi R, Whitehead R, Imamura M. Conditional transformation of mouse pancreatic epithelial cells: An in vitro model for analysis of genetic events in pancreatocarcinogenesis. Biochem Biophys Res Commun 2004. In press.
5. Fujimoto K, Sheng H, Shao J, Beauchamp RD. Transforming growth factor-beta1 promotes invasiveness after cellular transformation with activated Ras in intestinal epithelial cells. Exp Cell Res 2001;266:239-49.
6. Brat DJ, Lillemoe KD, Yeo CJ, Warfield PB, Hruban RH. Progression of pancreatic intraductal neoplasias to infiltrating adenocarcinoma of the pancreas. *Am J Surg* Pathol 1998;22:163-9.
7. Oft M, Peli J, Rudaz C, Schwarz H, Beug H, Reichmann E. TGF-beta1 and Ha-Ras collaborate in modulating the phenotypic plasticity and invasiveness of epithelial tumor cells. Genes Dev 1996;10:2462-77.
8. Kazbay K, Tarnasky PR, Hawes RH, Cotton PB. Increased transforming growth factor beta in pure pancreatic juice in pancreatitis. Pancreas 2001;22:193-5.
9. Satoh K, Shimosegawa T, Hirota M, Koizumi M, Toyota T. Expression of transforming growth factor beta1 (TGFbeta1) and its receptors in pancreatic duct cell carcinoma and in chronic pancreatitis. Pancreas 1998;16:468-74.
10. Apple SK, Hecht JR, Lewin DN, Jahromi SA, Grody WW, Nieberg RK. Immunohistochemical evaluation of K-ras, p53, and HER-2/neu expression in hyperplastic, dysplastic, and carcinomatous lesions of the pancreas: evidence for multistep carcinogenesis. Hum Pathol 1999;30:123-9.
11. Lehmann K, Janda E, Pierreux CE, Rytomaa M, Schulze A, McMahon M, et al. Raf induces TGFbeta production while blocking its apoptotic but not invasive responses: a mechanism leading to increased malignancy in epithelial cells. Genes Dev 2000;14:2610-22.
12. Hu PP, Datto MB, Wang XF. Molecular mechanisms of transforming growth factor-beta signaling. Endocr Rev 1998;19:349-63.

13. Datto MB, Li Y, Panus JF, Howe DJ, Xiong Y, Wang XF. Transforming growth factor beta induces the cyclin-dependent kinase inhibitor p21 through a p53-independent mechanism. Proc Natl Acad Sci U S A 1995;92:5545-9.
14. Cui W, Fowlis DJ, Bryson S, Duffie E, Ireland H, Balmain A, et al. TGFbeta1 inhibits the formation of benign skin tumors, but enhances progression to invasive spindle carcinomas in transgenic mice. Cell 1996;86:531-42.
15. Muraoka RS, Dumont N, Ritter CA, Dugger TC, Brantley DM, Chen J, et al. Blockade of TGF-beta inhibits mammary tumor cell viability, migration, and metastases. J Clin Invest 2002;109:1551-9.
16. Tang B, de Castro K, Barnes HE, Parks WT, Stewart L, Bottinger EP, et al. Loss of responsiveness to transforming growth factor beta induces malignant transformation of nontumorigenic rat prostate epithelial cells. Cancer Res 1999;59:4834-42.
17. Derynck R, Akhurst RJ, Balmain A. TGF-beta signaling in tumor suppression and cancer progression. Nat Genet 2001; 29:117-29.
18. Hahn SA, Hoque AT, Moskaluk CA, da Costa LT, Schutte M, Rozenblum E, et al. Homozygous deletion map at 18q21.1 in pancreatic cancer. Cancer Res 1996;56: 490-4.

Analysis of E-, N-Cadherin, α-, β-, and γ-Catenin Expression in Human Pancreatic Carcinoma Cell Lines

Eiji Toyoda, MD, Ryuichiro Doi, MD, Masayuki Koizumi, MD, Kazuhiro Kami, MD, Daisuke Ito, MD, Tomohiko Mori, MD, Koji Fujimoto, MD, Sanae Nakajima, MD, Michihiko Wada, MD, and Masayuki Imamura, MD

Objectives: Cadherins are cell surface glycoproteins that mediate Ca^{2+}-dependent, homophilic cell-cell adhesion. The classic cadherins interact with either β-catenin or γ-catenin, which is bound to α-catenin that links the complex to the actin cytoskeleton. It has been reported that alteration in cadherins/catenins function or expression is found in the neoplastic process as a step in metastasis. The aim of this study was to analyze the expressions of E- and N-cadherins and catenins in human pancreatic cancer cell lines.

Methods: We examined the expression of cadherins and catenins in 7 human pancreatic cancer cells by RT-PCR, Western blotting, and immunocytochemistry. The interactions between cadherins and β-catenin were assessed by immunoprecipitation.

Results: E-cadherin was expressed in all cell lines except for MIAPaCa-2, whereas N-cadherin was expressed in Capan-2, CFPAC-1, BxPC-3, and PANC-1. The α-, β-, and γ-catenins were expressed and cadherins/β-catenin interactions were detected in all cadherin-expressing cells. Immunocytochemical analysis showed membranous expression of cadherins and catenins.

Conclusion: The decreased or loss of cadherins and catenins expression could be involved in the tumor progression and metastasis, although these events may occur in in vivo conditions by interaction between cancer cells and extracellular matrices.

Key Words: pancreatic cancer, cadherin, catenin

(*Pancreas* 2005;30:168–173)

Invasion and metastasis can be facilitated by proteins that stimulate tumor cell attachment to host cellular or extracellular matrix determinants, tumor cell proteolysis of host barriers, such as the basement membrane, tumor cell locomotion, and tumor cell colony formation in the target organ for metastasis.[1] It is known that cadherins are major cell-cell adhesion molecules in tumors as well as in normal tissues. The perturbation of cadherin function causes temporal or permanent disaggregation of tumor cells and may thus promote the invasion and metastasis of such cells.[2]

E-cadherin is a member of a family of Ca^{2+}-dependent integral membrane cell-cell adhesion receptors.[3] E-cadherin is localized at the zonula adherens junction between epithelial cells[4] and is associated with peripheral basal-lateral actin filaments in a multiprotein complex with kinases, phosphatases, and catenins.[5] The cytoplasmic complex, which anchors E-cadherin to the actin cytoskeleton,[6] includes the intracellular proteins α-catenin, which has homology to vinculin,[7] and the armadillo family members β-catenin and γ-catenin.[8] After cell-cell contact, adhesion of the E-cadherin/catenin complex functions to establish epithelial cellular architecture by initiating formation of desmosomes, tight junctions, and gap junctions.[9]

Alteration in E-cadherin/catenin function or expression is found in the neoplastic process as a step in metastasis.[10] The loss of E-cadherin/catenin function results, in part, in a transformation from the normal epithelioid morphology toward an invasive and less differentiated mesenchymal phenotype.[11] Immunohistochemical analysis of highly invasive tumors (breast, melanoma, prostate, non-small cell lung carcinomas) indicates that these tissues have decreased E-cadherin levels, suggesting a decreased function for E-cadherin in organization of tissue structure.[12]

Interestingly, recent studies have reported that N-cadherin, one of the mesenchymal cadherins, enhances tumor cell motility and migration,[13,14] thus showing an opposite effect as compared with E-cadherin. N-cadherin–induced tumor cell invasion can even overcome E-cadherin–mediated cell-cell adhesion.[13,15] Furthermore, N-cadherin is expressed in human tumors that have lost E-cadherin expression.[16,17]

As for the pancreatic cancer cells, the loss of membranous E-cadherin expression is associated with high grade and advanced stage in pancreatic cancer.[18] However, it is not known whether the aforementioned "cadherin switch" is involved in the neoplastic and invasive progression of pancreatic cancer cells. The current study was conducted to investigate the full spectrum of the cadherin/catenin expression in human pancreatic cancer cell lines at the level of messenger RNAs and proteins.

Received for publication June 2, 2004; accepted August 30, 2004.
From Department of Surgery and Surgical Basic Science, Kyoto University, Kyoto, Japan.
Supported by a Grant-in-Aid (#15390395) from the Ministry of Education of Japan.
Reprints: Ryuichiro Doi, MD, Department of Surgery and Surgical Basic Science, Kyoto University, 54 Shogoinkawaracho, Sakyo, Kyoto 606-8507, Japan (e-mail: doir@kuhp.kyoto-u.ac.jp).

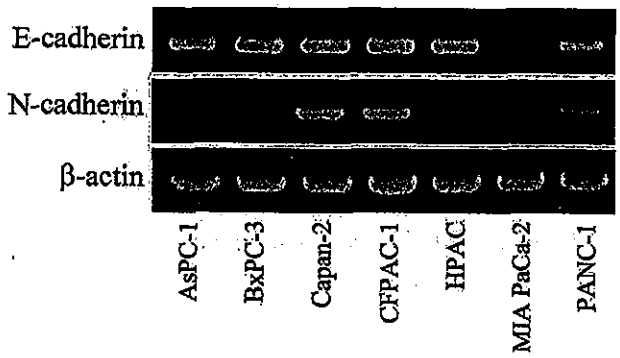

FIGURE 1. E- and N-cadherin mRNA expression in human pancreatic cancer cells. E-cadherin mRNA was detected in all cell lines except for MIAPaCa-2. N-cadherin m-RNA was detected in BxPC-3, Capan-2, CFPAC-1, and PANC-1.

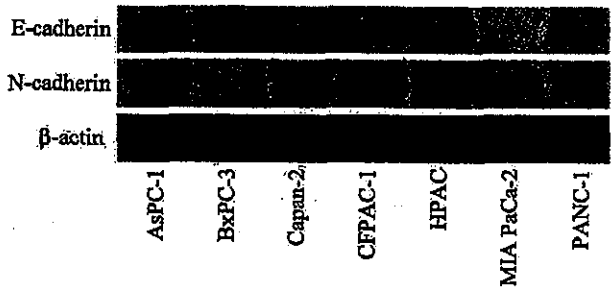

FIGURE 2. E- and N-cadherin protein expression in human pancreatic cancer cells. E-cadherin protein was detected in all cell lines except for MIAPaCa-2. N-cadherin protein was detected in BxPC-3, Capan-2, CFPAC-1, and PANC-1.

METHODS

Cell Line and Culture Conditions

Human pancreatic cancer cell lines (AsPC-1, BxPC-3, Capan-2, CFPAC-1, HPAC, MIAPaCa-2, and PANC-1) were maintained in the following media at 37°C in a humid atmosphere of 5% CO_2/95% air. AsPC-1 cells, BxPC-1 cells, and HPAC cells were cultured in RPMI 1640 medium (Gibco-BRL, Grand Island, NY) with 10% fetal bovine serum (FBS) (ICN Biomedicals, Aurora, OH). CAPAN-2 cells, CFPAC-1 cells, MIAPaCa-2 cells, and PANC-1 cells were cultured in medium recommended by American Type Culture Collection. Each medium contained 100 U/mL penicillin and 0.1 mg/mL streptomycin (Gibco-BRL).

Antibodies

The mouse monoclonal anti-N-cadherin antibody and mouse monoclonal anti-β-catenin antibody were purchased from Zymed Laboratories Inc. (South San Francisco, CA). The mouse monoclonal anti–α-catenin antibody and mouse monoclonal anti–γ-catenin antibody were purchased from Transduction Laboratories (Lexington, KY). The mouse monoclonal anti–β-actin antibody (clone AC-15) was purchased from Sigma (St. Louis, MO). The biotinylated secondary antibody (goat anti-mouse IgG) used immunocytochemistry procedures was purchased from Jackson Immuno Research Laboratories (West Grove, PA). For immunoblotting, the horseradish peroxidase–conjugated antibody was HRP-gout anti-mouse IgG (Zymed Laboratories).

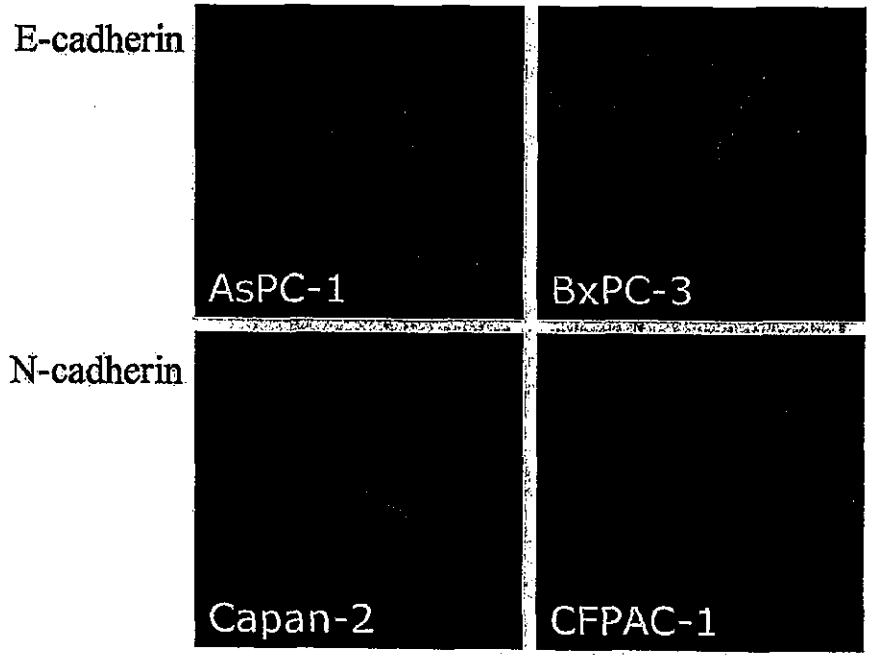

FIGURE 3. Immunocytochemical detection of E- and N-cadherins. Typical staining of E-cadherin and N-cadherin shows a membranous expression.

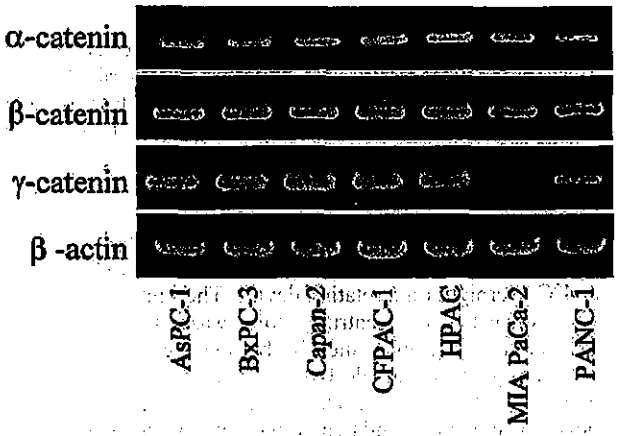

FIGURE 4. α-, β-, and γ-catenin mRNA expression in human pancreatic cancer cells. The mRNA expression of α-, β-, and γ-catenins was detected in all cell lines. However, the expression of γ-catenin in MIAPaCa-2 is extremely low.

Reverse Transcriptase Polymerase Chain Reaction (RT-PCR)

Total cellular RNA was prepared using TRIZOL Reagent (Life Technologies, Rockville, MD) and cDNA was prepared by random priming from 1 μg of total RNA using a First-Strand cDNA Synthesis kit (Pharmacia Biotech, North Peapack, NJ) according to the manufacturer's instructions. Five microliters of first-strand cDNA solution was subjected to PCR with synthetic oligonucleotide primers (NIPPON EGT, Toyama, Japan). The sequences for the primers used in this study are as follows:

E-cadherin upstream: 5′-TCCATTTCTTGGTCTACGCC-3′,
downstream: 5′-CACCTTCAGCCATCCTGTTT-3′
N-cadherin upstream: 5′-GTGCCATTAGCCAAGGGAATT-CAGC-3′,
downstream: 5′-GCGTTCCTGTTCCACTCATAGGAGG-3′
α-catenin upstream: 5′-GTCATTCACGTAGTCACCTCA-3′,
downstream: 5′-TTCTGACATCAAAATCTTCTGTC-3′
β-catenin upstream: 5′-AAGGTCTGAGGAGCAGCTTC-3′,
downstream: 5′-TGGACCATAACTGCAGCCTT-3′
γ-catenin upstream: 5′-ATGGAGGTGATGAACCTGATGG-3′,
downstream: 5′-CCTGACACACCAGGGCACAT-3′
β-actin upstream: 5′-GGCATCGTGATGGACTCCG-3′,
downstream: 5′-GCTGGAAGGTGGACAGCGA-3′

The products were 361, 369, 301, 668, 284, and 613 base pairs, respectively.

The reproducibility of the technique and quality of the total RNA were confirmed using β-actin primers. Specific sequences were amplified by 30 cycles (30 seconds of denaturation at 94°C, 30 seconds annealing at 60°C, and 1 minute extension at 72°C), followed by a final incubation at 72°C for 10 minutes. PCR products were analyzed on a 2% agarose gel.[19]

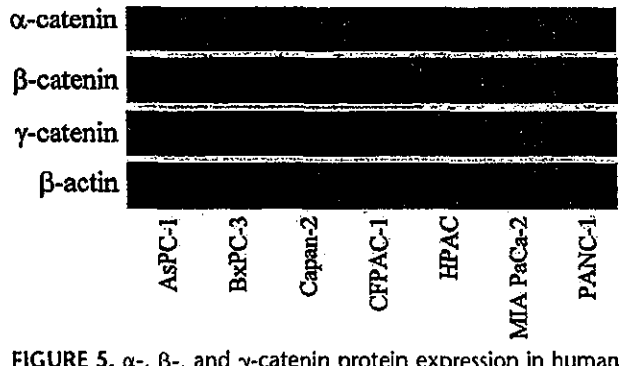

FIGURE 5. α-, β-, and γ-catenin protein expression in human pancreatic cancer cells. α-, β-, and γ-catenin protein was detected in these cells except MIAPaCa-2. No protein expression of β-catenin was found in MIAPaCa-2.

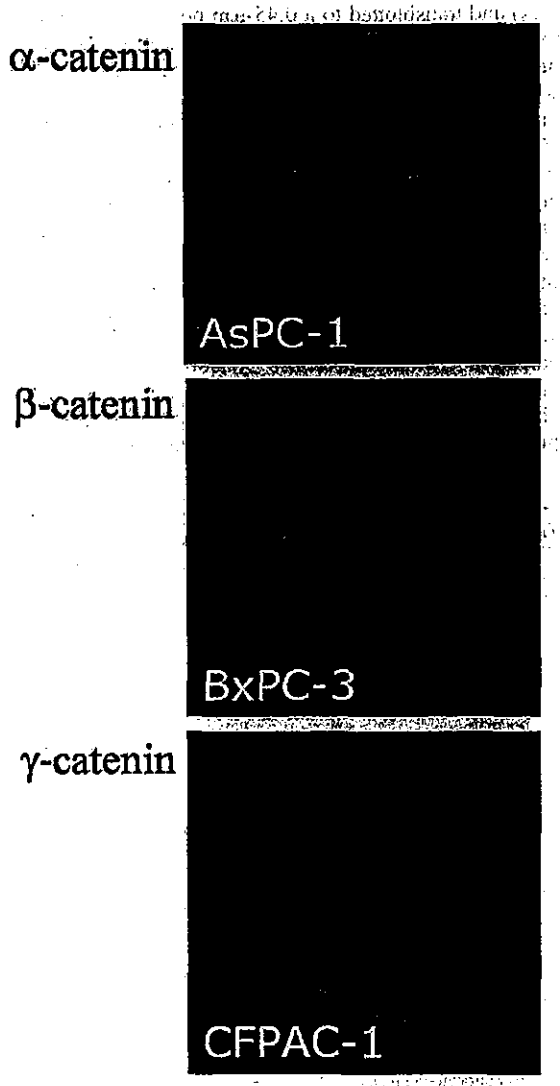

FIGURE 6. Immunocytochemical detection of α-, β-, and γ-catenins. Typical staining of α-, β-, and γ-catenins shows a membranous expression.

Western Blot Analysis

Cells were lysed in RIPA buffer containing 50 mmol/L HEPES (pH 7.0), 250 mmol/L NaCl, 0.1% Nonidet P-40, 1 mmol/L phenylmethylsulfonylfluoride (PMSF), and 20 μg/mL gabexate mesylate and incubated on ice for 10 minutes; then the lysate was sonicated for 10 seconds. Total extracts were cleaned by centrifugation at 15,000 rpm for 10 minutes at 4°C, and the supernatants were collected. Protein concentration was measured by a BCA protein assay reagent (Pierce, Rockford, IL). The lysates were resuspended in 1 volume of the gel loading buffer that contained 50 mmol/L Tris-HCl (pH 6.7), 4% SDS, 0.02% bromophenol blue, 20% glycerol, and 4% 2-mercaptoethanol and then heated at 95°C for 5 minutes. The extracted protein was subjected to Western blotting. In brief, 50 μg aliquots of protein was size-fractionated to a single dimension by SDS-PAGE (6%–10% gels) and transblotted to a 0.45-μm polyvinylidene difluoride membrane (IPVH304F0, Millipore, Billerica, MA) in a semi-dry electroblot apparatus (Bio-Rad, Richmond, CA). The blots were then washed 3 times in TBS with 0.1% Tween-20 (TBST) and incubated for 1 hour at room temperature in blocking buffer (Block Ace, Dainipponseiyaku, Osaka, Japan). Subsequently, the blots were immunoblotted with an appropriate primary antibody for 1 hour at room temperature or overnight at 4°C. Unbound antibody was removed by washing the membrane with TBST 3 times, each 10 minutes. The membrane was then incubated with a horseradish peroxidase–conjugated secondary antibody for 1 hour at room temperature followed by an addition of TBST. Antibody reaction was detected by the enhanced chemiluminescence system (Amersham, Buckinghamshire, UK). The membranes were treated with enhanced chemiluminescence reagents according to the manufacturer's protocol and were exposed to x-ray films for 5–120 seconds.

Immunoprecipitation

For immunoprecipitation of cadherin-catenin complexes, total cell lysate were obtained as described above. To remove nonspecifically bound material, cell lysates (about 1 mg of protein) were precleared by incubation with 0.25 μg of normal mouse IgG (Santa Cruz Biotechnology, Santa Cruz, CA.), together with 20 μL of Protein G PLUS-Agarose (Santa Cruz) for 30 minutes at 4°C. After centrifugation, the supernatants were incubated with primary antibody for 2 hours at 4°C and then with 20 μL of protein G PLUS-Agarose at 4°C overnight on a rotating device. The immunocomplexes were collected by centrifugation, washed 4 times with extraction buffer, and eluted by boiling the beads in 40 μL of electrophoresis sample buffer (sc-24945, Santa Cruz) for 3 minutes. Immunoprecipitates were separated on SDS-8% polyacrylamide gels and transferred onto membranes. Western blots were further processed as described above.

Immunocytochemistry

Pancreatic cancer cells were seeded on coverslips and incubated for 24 hours at 37°C in a humid atmosphere of 5% CO_2/95% air. The coverslips with cells were then fixed with 4% paraformaldehyde in PBS for 10 minutes, washed with PBS, permeabilized in 1% Triton X-100 in PBS for 15 minutes, washed, and blocked with TBST with 1% BSA. Fixed and permeabilized cells were incubated with an appropriate primary antibody diluted in 1% BSA-TBST (v/wk) for 2 hours at 37°C, and rinsed 3 times with TBST, and then incubated for 30 minutes with Cy3-conjugated Affinipure goat anti-mouse IgG diluted in 1% BSA-TBST (v/wk). After the final wash, coverslips were mounted on the slide glass with Vectashield mounting medium (Vector Laboratories, Burlingame, CA).

TABLE 1. Expression of E-, N-cadherin, α-, β-, and γ-Catenin Expression in Human Pancreatic Adenocarcinoma

	AsPC-1	BxPC-3	Capan-2	CFPAC-1	HPAC	MIA PaCa-2	PANC-1
E-cadherin							
RT-PCR	+	+	+	+	+	−	+
Western blotting	+	++	+	++	++	−	+
Immunocytochemistry	+	+	+	+	+	−	+
N-Cadherin							
RT-PCR	−	±	+	+	−	−	+
Western blotting	−	±	++	++	−	−	+
Immunocytochemistry	−	−	+	+	−	−	+
α-catenin							
RT-PCR	+	+	+	+	+	+	+
Western blotting	+	+	+	+	+	±	+
β-catenin							
RT-PCR	+	+	+	+	+	+	+
Western blotting	++	++	++	++	++	−	++
Immunocytochemistry	+	+	+	+	+	UT	+
γ-catenin							
RT-PCR	+	+	+	+	+	±	+
Western blotting	++	++	++	++	+	±	++
Immunocytochemistry	+	+	+	+	+	UT	+

++, strong expression; +, positive expression; ±, weak expression; −, negative expression; UT, untried.

The cells were examined under a fluorescein microscope (Olympus, Tokyo, Japan).

RESULTS

The expression of cadherins in human pancreatic cancer cell lines was performed by 3 accepted techniques for gene expression. Figure 1 shows the mRNA expression of E-cadherin and N-cadherin. E-cadherin mRNA was detected in all cell lines except for MIAPaCa-2. N-cadherin mRNA was detected in BxPC-3, Capan-2, CFPAC-1, and PANC-1. The protein expression of E-cadherin and N-cadherin was measured by Western blot analysis (Fig. 2). The results of protein expression were identical to the mRNA expression for each protein. Figure 3 shows the typical staining of E-cadherin and N-cadherin. Both E-cadherin and N-cadherin were detected as a membranous protein. Immunocytochemical detection of E-cadherin and N-cadherin was consistent with the expression of mRNA and protein.

We next measured the expression of catenins in human pancreatic cancer cells. The mRNA expression of α-, β-, and γ-catenins was detected in all cell lines that we examined. However, the expression of γ-catenin in MIAPaCa-2 was extremely low (Fig. 4). Protein expression of catenins was similar to the mRNA expression in these cells except MIAPaCa-2. No protein expression of β-catenin was found in MIAPaCa-2, although it expressed β-catenin at the mRNA level (Fig. 5). Immunocytochemical detection of α-, β-, and γ-catenins showed membranous expression (Fig. 6). The results were summarized in Table 1. E-cadherin/β-catenin interaction was detected in all cell lines except MIAPaCa-2 (Fig. 7A), whereas N-cadherin/β-catenin interaction was detected in N-cadherin–expressing cells (Fig. 7B).

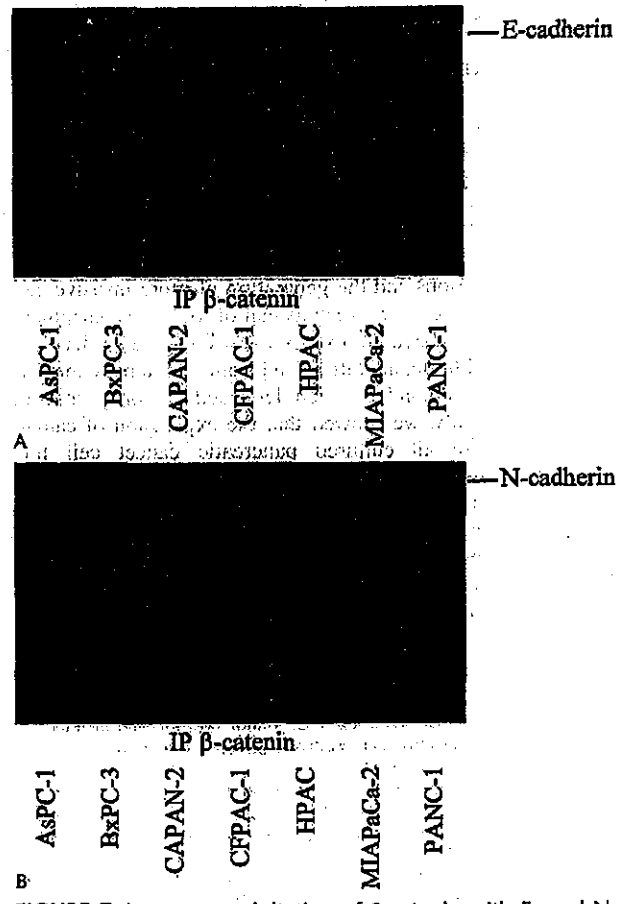

FIGURE 7. Immunoprecipitation of β-catenin with E- and N-cadherin. Equal amounts of proteins from each cell line were immunoprecipitated (IP) with antibody against β-catenin. Immunoprecipitates were separated by SDS-PAGE, transferred onto membranes, and immunoblotted with E-cadherin (A) and N-cadherin (B). Efficiency of immunoblot reaction and molecular weight of each detected protein were verified by loading 25 μg of CFPAC protein lysate. E-cadherin/β-catenin interaction was detected in all cell lines except MIAPaCa-2, whereas N-cadherin/β-catenin interaction was detected in N-cadherin–expressing cells. The IgG heavy and light chains recognized by secondary antibodies are visible at the bottom of the gel.

DISCUSSION

Pignatelli et al[18] reported that loss of normal surface E-cadherin expression was found in 19 of 36 (53%) pancreatic cancer tumors compared with the adjacent normal ductal cells. Abnormal E-cadherin expression was found more frequently in poorly differentiated than in well-differentiated tumors. Membranous E-cadherin expression was also lost more frequently in primary tumors with lymph node and distant metastasis compared with lymph node–negative tumors. Based on these observations, they suggested that the loss of membranous E-cadherin expression is associated with high grade and advanced stage in pancreatic cancer. Therefore, we thought that a considerable number of cell lines would show a decreased or loss of E-cadherin expression. However, contrary to our expectation, we found that E-cadherin is expressed in 6 of 7 pancreatic cancer cell lines at levels of both mRNA and protein.

Among the pancreatic adenocarcinoma cell lines that were tested in this study, AsPC-1 is derived from the ascites of a patient with cancer of the pancreas,[20] and CFPAC-1 is from the liver metastasis of ductal carcinoma.[21] Other cell lines were derived from human pancreatic ductal carcinomas. We found decreased expression of E-cadherin in MIAPaCa-2. However, there were no differences in expression tendency between cell lines from primary tumors and those from ascites and metastasis. Therefore, we speculate that the decreased or loss of E-cadherin expression in excised pancreatic cancer tissue could be an in vivo event that is affected by surrounding tissues such as the extracellular matrix component.

N-cadherin expression was detected in 4 cell lines (BxPC-3, Capan-2, CFPAC-1, PANC-1). CFPAC-1, derived from liver metastasis, demonstrated the strongest expression of N-cadherin. The result is in accordance with the cadherin switch theory. However, AsPC-1 that is derived from ascites did not express N-cadherin mRNA or protein. Capan-2 derived from the primary pancreatic cancer tumor showed strong

N-cadherin expression. Therefore, we did not find E-cadherin and N-cadherin conversion, at least, in our observations in vitro. Therefore, similar to the results of E-cadherin, the cadherin switch from epithelial to mesenchymal cadherins would be an in vivo phenomenon.

The cytoplasmic domain of E-cadherin interacts with intracellular proteins called α-, β-, and γ-catenins, which make contact with the microfilament network.[22] Catenins are essential for E-cadherin function, and alterations in expression or structure of the catenins may lead to the disassembly of adherens junctions and the generation of more invasive cells. In some human cancers, such as that of the breast, esophagus, and prostate, decreased expression of α-catenin has been noted.[23] In addition, alterations in β- and γ-catenin expression and phosphorylation have been described for some tumor cell lines.[24,25] Finally, we showed that the expression of catenins was found in all cultured pancreatic cancer cell lines. Therefore, the expression of catenins in pancreatic cancer cells was not altered in in vitro conditions. In conclusion, as suggested previously, the decreased or loss of cadherins and catenins expression could be involved in the tumor progression and metastasis, although these events may occur in in vivo conditions by interaction between cancer cells and extracellular matrices.

REFERENCES

1. Liotta LA, Stetler-Stevenson WG. Tumor invasion and metastasis: an imbalance of positive and negative regulation. *Cancer Res.* 1991;51(18 suppl):5054s–5059s.
2. Takeichi M. Cadherins in cancer: implications for invasion and metastasis. *Curr Opin Cell Biol.* 1993;5:806–811.
3. Takeichi M. Morphogenetic roles of classic cadherins. *Curr Opin Cell Biol.* 1995;7:619–627.
4. Rajasekaran AK, Hojo M, Huima T, et al. Catenins and zonula occludens-1 form a complex during early stages in the assembly of tight junctions. *J Cell Biol.* 1996;132:451–463.
5. Ozawa M, Baribault H, Kemler R. The cytoplasmic domain of the cell adhesion molecule uvomorulin associates with three independent proteins structurally related in different species. *EMBO J.* 1989;8:1711–1717.
6. Nagafuchi A, Shirayoshi Y, Okazaki K, et al. Transformation of cell adhesion properties by exogenously introduced E-cadherin cDNA. *Nature.* 1987;329:341–343.
7. Herrenknecht K, Ozawa M, Eckerskorn C, et al. The uvomorulin-anchorage protein alpha catenin is a vinculin homologue. *Proc Natl Acad Sci U S A.* 1991;88:9156–9160.
8. McCrea PD, Turck CW, Gumbiner B. A homolog of the armadillo protein in Drosophila (plakoglobin) associated with E-cadherin. *Science.* 1991; 254:1359–1361.
9. Boller K, Vestweber D, Kemler R. Cell-adhesion molecule uvomorulin is localized in the intermediate junctions of adult intestinal epithelial cells. *J Cell Biol.* 1985;100:327–332.
10. Schipper JH, Frixen UH, Behrens J, et al. E-cadherin expression in squamous cell carcinomas of head and neck: inverse correlation with tumor dedifferentiation and lymph node metastasis. *Cancer Res.* 1991; 51:6328–6337.
11. Birchmeier C, Birchmeier W, Brand-Saberi B. Epithelial-mesenchymal transitions in cancer progression. *Acta Anat (Basel).* 1996;156:217–226.
12. Giroldi LA, Schalken JA. Decreased expression of the intercellular adhesion molecule E-cadherin in prostate cancer: biological significance and clinical implications. *Cancer Metastasis Rev.* 1993;12:29–37.
13. Hazan RB, Phillips GR, Qiao RF, et al. Exogenous expression of N-cadherin in breast cancer cells induces cell migration, invasion, and metastasis. *J Cell Biol.* 2000;148:779–790.
14. Li G, Satyamoorthy K, Herlyn M. N-cadherin-mediated intercellular interactions promote survival and migration of melanoma cells. *Cancer Res.* 2001;61:3819–3825.
15. Nieman MT, Prudoff RS, Johnson KR, et al. N-cadherin promotes motility in human breast cancer cells regardless of their E-cadherin expression. *J Cell Biol.* 1999;147:631–644.
16. Li G, Herlyn M. Dynamics of intercellular communication during melanoma development. *Mol Med Today.* 2000;6:163–169.
17. Tomita K, van Bokhoven A, van Leenders GJ, et al. Cadherin switching in human prostate cancer progression. *Cancer Res.* 2000;60:3650–3654.
18. Pignatelli M, Ansari TW, Gunter P, et al. Loss of membranous E-cadherin expression in pancreatic cancer: correlation with lymph node metastasis, high grade, and advanced stage. *J Pathol.* 1994;174:243–248.
19. Mialhe A, Levacher G, Champelovier P, et al. Expression of E-, P-, n-cadherins and catenins in human bladder carcinoma cell lines. *J Urol.* 2000;164:826–835.
20. Chen WH, Horoszewicz JS, Leong SS, et al. Human pancreatic adenocarcinoma: in vitro and in vivo morphology of a new tumor line established from ascites. *In Vitro.* 1982;18:24–34.
21. Schoumacher RA, Ram J, Iannuzzi MC, et al. A cystic fibrosis pancreatic adenocarcinoma cell line. *Proc Natl Acad Sci U S A.* 1990;87:4012–4016.
22. Kemler R. From cadherins to catenins: cytoplasmic protein interactions and regulation of cell adhesion. *Trends Genet.* 1993;9:317–321.
23. Morton RA, Ewing CM, Nagafuchi A, et al. Reduction of E-cadherin levels and deletion of the alpha-catenin gene in human prostate cancer cells. *Cancer Res.* 1993;53:3585–3590.
24. Sommers CL, Gelmann EP, Kemler R, et al. Alterations in beta-catenin phosphorylation and plakoglobin expression in human breast cancer cells. *Cancer Res.* 1994;54:3544–3552.
25. Behrens J, Vakaet L, Friis R, et al. Loss of epithelial differentiation and gain of invasiveness correlates with tyrosine phosphorylation of the E-cadherin/beta-catenin complex in cells transformed with a temperature-sensitive v-SRC gene. *J Cell Biol.* 1993;120:757–766.

Original Paper

Pathobiology

Pathobiology 2004;71:26–34
DOI: 10.1159/000072959

Received: January 16, 2003
Accepted: March 18, 2003

Association between Expression Levels of CA 19-9 and *N-Acetylglucosamine-β1,3-Galactosyltransferase 5* Gene in Human Pancreatic Cancer Tissue

Nobuyasu Hayashi[a] Shoji Nakamori[a] Jiro Okami[a] Hiroaki Nagano[a] Keizo Dono[a] Koji Umeshita[a] Masato Sakon[a] Hisashi Narimatsu[b] Morito Monden[a]

[a]Department of Surgery and Clinical Oncology, Graduate School of Medicine, Osaka University, Osaka, and [b]Division of Cell Biology, Institute of Life Science and Department of Bioengineering, Faculty of Engineering, Soka University, Tokyo, Japan

Key Words
CA 19-9 · DUPAN-2 · β3Gal-T5 · Gene expression · Quantification · Immunoreactivity

Abstract
Objective: CA 19-9, equivalent to Sialyl Lewis[a] antigen, is a well-known tumor marker in pancreatic cancer. At the initial step of the biosynthesis of CA 19-9, N-acetylglucosamine-β1,3-galactosyltransferase (β3Gal-T) transfers galactose to N-acetylglucosamine (GlcNAc). Recently, β3Gal-T5 has been presumed to be related to the formation of the type 1 chain in an in vitro experiment in terms of kinetic enzyme characterization. The purpose of this study was to investigate which β3Gal-T is related to the synthesis of CA 19-9 in human pancreatic cancer tissues. ***Methods:*** We examined *β3Gal-T1, T2, T3, T4,* and *β3Gal-T5* mRNA expressions in 13 noncancerous and cancerous tissues of the human pancreas using real-time polymerase chain reaction, and compared those gene expression levels with the immunoreactivity of CA 19-9 and its precursor DUPAN-2 in cancerous tissues. ***Results:*** *β3Gal-T5* gene expression significantly augmented in cancerous tissues, when compared with the adjacent noncancerous tissues. Additionally, there was a good correlation between *β3Gal-T5* gene transcription levels and immunohistochemical grades of CA 19-9 or its precursor DUPAN-2 in cancerous tissues. However, no correlation was observed between *β3Gal-T1, T2, T3,* and *β3Gal-T4* gene expression levels and CA 19-9 or DUPAN-2 immunoreactive grades in cancerous tissue. ***Conclusion:*** β3Gal-T5 is presumed to be responsible for the synthesis of CA 19-9 in pancreatic cancer tissue.

Introduction

Aberrant glycosylation in cell surface membranes is one of the most common characteristics during the malignant transformation and tumor progression [1, 2]. Since the application of monoclonal antibody techniques in the late 1970s, many aberrant glycosylation products on the membrane have been identified as tumor-associated carbohydrates [3]. These carbohydrate antigens have been widely utilized as tumor markers for cancer patients to

KARGER
Fax + 41 61 306 12 34
E-Mail karger@karger.ch
www.karger.com

1015–2008/04/0711–0026$21.00/0

Accessible online at:
www.karger.com/pat

Dr. Shoji Nakamori
Department of Surgery and Clinical Oncology
Graduate School of Medicine, Osaka University
E2, 2-2 Yamadaoka, Suita, Osaka 565-0871 (Japan)
Tel. +81 6 6879 3251, Fax +81 6 6879 3259, E-Mail nakamori@surg2.med.osaka-u.ac.jp

survey or monitor the disease. Furthermore, recent biochemical and biological studies have indicated that some of these antigens in the cancer cell membrane affect tumor activities, such as adhesion [2], motility [1, 2], immunogenicity and other immune recognition processes [4], or invasive characteristics [5]. Among these carbohydrate antigen epitopes, Sialyl Lewis^a (sLe^a) is detected by the 1116NS19-9 monoclonal antibody, and termed as CA 19-9 [6]. It is well known as a reliable and sensitive serum tumor marker of pancreatic cancer [7] because it exhibits appropriate sensitivity and specificity for the serological detection of this disease [8]. Increased serum level of CA 19-9 is associated with poor prognosis not only in pancreatic cancer [9], but also in gastric [10] or colorectal cancer [11]. Several studies have demonstrated the relation between increased CA 19-9 expression in the primary cancerous tissues and worse prognostic significance in those cancers [12, 13]. However, in spite of these clinical observations or speculations, the exact mechanism of the altered expression of CA 19-9 in the cancerous tissues has not been well elucidated.

According to the pathways proposed in figure 1, which are presumed to function in digestive organ epithelial cells, the synthesis of the sLe^a epitope at the terminal end of carbohydrate chains requires a set of several glycosyltransferases [14]. Three glycosyltransferases, i.e. N-acetylglucosamine-β1,3-galactosyltransferase (β3Gal-T), galactose-α2,3-sialyltransferase (ST3Gal) and α1,3/4-fucosyltransferase (Fuc-TIII), are involved in the formation of sLe^a (CA 19-9) in colorectal cancer. First, β3Gal-T transfers galactose (Gal) to N-acetylglucosamine (GlcNAc) with a β1,3-linkage, leading to the synthesis of Galβ1,3GlcNAc, the type 1 chain. Next, ST3Gal transfers sialic acid (SA) to the Gal residue of the type 1 chain with an α2,3-linkage, resulting in SAα2,3Galβ1,3GlcNAc, sLe^c or DUPAN-2. Finally, the Lewis (Le) enzyme, Fuc-TIII, transfers fucose (Fuc) to the GlcNAc residue of the sLe^c with an α1,4-linkage to complete the synthesis of sLe^a, CA 19-9 (fig. 1).

A recent study has demonstrated that the amount of terminal carbohydrate epitopes, such as CA 19-9, is not necessarily determined by the terminal glycosyltransferase, such as the Le enzyme, but is rather controlled by more upstream glycosyltransferases, such as ST3Gals or β3Gal-Ts [15]. In our previous study, an appropriate correlation between the Le enzyme or ST3Gals and CA 19-9 expression has not been observed in pancreatic cancer [16].

To date, various members of *β3Gal-T* genes were cloned through the application of an EST cloning strategy

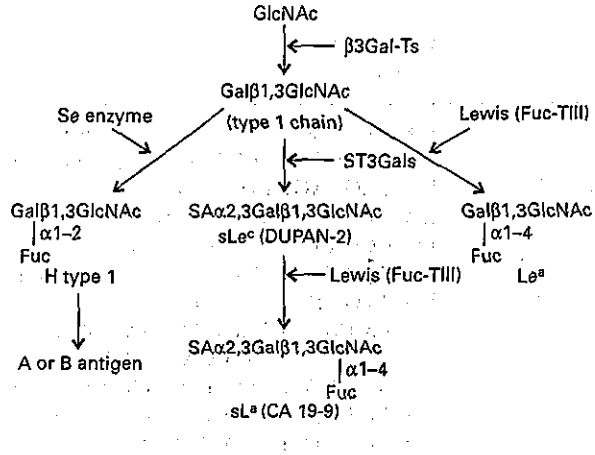

Fig. 1. Biosynthetic pathway showing the relationship among β3Gal-Ts, type 1 chain, CA 19-9 and DUPAN-2.

[17–20]. One of the β3Gal-T members, β3Gal-T5, has been demonstrated to be the possible key enzyme responsible for the synthesis of the type 1 chain, which leads to the formation of CA 19-9 using various cancer cell lines [20, 21]. Although the formation of the carbohydrate antigen is attributed to the regulated expression of a certain glycosyltransferase gene involved in the cascade of the synthesis [5], alteration of the message levels of these *β3Gal-T* genes has not been well studied, especially in human pancreatic cancer. In the present study, we investigated the involvement of gene expressions of representative *β3Gal-T* members, i.e. *β3Gal-T1, T2, T3, T4,* and *β3Gal-T5* for the synthesis of CA 19-9 in pancreatic cancer tissues.

Materials and Methods

Patients and Tissue Specimen

After informed consent had been obtained, 13 patients with invasive pancreatic duct cell carcinomas who had undergone curative resection between March 1998 and August 1999 at the Department of Surgery and Clinical Oncology, Graduate School of Medicine, Osaka University, Osaka, Japan, were enrolled in this study. Resected specimens from the 13 patients were examined macroscopically and microscopically to determine the location of tumor, tumor size, extent and mode of cancer invasion, metastasis to lymph node and histological type. The mean age of the patients was 65 years, ranging from 45 to 72 years. Seven patients were male and 6 patients were female. Eleven tumors were located in the head of the pancreas and 2 in the body and tail. The disease stage was classified according to the international TNM staging system [22]. Paired tissues from

Table 1. Oligonucleotide primers used for the cloning of glycosyltransferase genes and PCR-RFLP for *Le* genotyping

RNA	Primer sets	Size of PCR products, bp	Annealing temperature, °C	Melting temperature, °C
β3Gal-T1	F:5′-TTCAGCCACCTAACAGTTGCCAGG-3′ R:5′-ATACCTTCTTCGTGGCTTGGTGGAG-3	495	56	85.2
β3Gal-T2	F:5′-TAGAAGCTAGAAGAGCTATTCGGC-3′ R:5′-ACTCGCCAGTGATTGAACACAAAC-3′	616	56	87.8
β3Gal-T3	F:5′-CCCAATGCCAAGTACGTAATGAAG-3′ R:5′-TGTGGTGTTCCTTAGCATGACCTG-3	474	56	81.7
β3Gal-T4	F:5′-TTGATCCCCAACCAGGAAGCTTGC-3′ R:5′-GCCACGATCCTGAAGAGGCA-3′	590	65	91.5
β3Gal-T5	F:5′-CAAACCAAGCCCAGAACCTG-3′ R:5′-TCAATCTCATCTTCGGGAAAGC-3′	153	58	81.5
PBGD	F:5′-TGTCTGGTAACGGCAATGCGGCTGCAAC-3′ R:5′-TCAATGTTGCCACCACACTGTCCGTCT-3	127	58	86.3
Primer for RFLP	F:5′-CCATGGCGCCGCTGTCTGGCCGCCC-3′ R:5′-AGTGGCATCGTCTCGGGACACACG-3′	93	62	

F = Forward primer; R = reverse primer.

each tissue sample, cancerous and adjacent noncancerous tissues, were immediately frozen into liquid nitrogen and stored at −80°C until RNA extraction. The other part of the paired tissues from each one was fixed in formalin and embedded in paraffin for routine pathologic examination and for CA 19-9 and DUPAN-2 immunohistostaining.

Genotyping of the Le *Gene*

The *Le* genotypes of the patients were determined by the polymerase chain reaction-restriction fragment length polymorphism (PCR-RFLP) method using genomic DNAs extracted from normal pancreas tissues. The method for *Le* genotyping by the detection of one mutation, T59G, was performed as described previously [23].

RNA Extraction and Complementary DNA Synthesis

Tissue specimens were minced with a disposable homogenizer (Edatm, Tokyo, Japan) in Trizol Reagent (Life Technologies, Vienna, Austria). RNA extraction was carried out according to the instructions provided by the supplier [24]. Purified RNA was quantified and assessed for purity by UV spectrophotometry. RNA samples were stored after being dissolved with diethyl pyrocarbonate-treated water. To remove contaminating genomic DNA, RNA was treated with RNase-free DNase (Promega, Madison, Wisc., USA). Complementary DNA (cDNA) was generated from 1 μg RNA with avian myeloblastosis virus reverse transcriptase (Promega, Madison, Wisc., USA), as described previously [24].

Real-Time Quantification PCR Assay with LightCycler™

Fluorescence PCR was performed using LightCycler (Idaho Technology, Salt Lake City, Utah, USA) [25], as described previously [26]. Briefly, a 10-μl PCR reaction contained 0.2 μ*M* of each primer (table 1), LC-DNA Master SYBR Green I (Boehringer Mannheim, Mannheim, Germany), 4 m*M* $MgCl_2$ and 2 μl of cDNA as a template. PCR conditions were set up as follows: 1 cycle of denaturing at 95°C for 2 min, followed by 40 cycles of 95°C for 0 s, each annealing temperature (table 2) for 5 s and 72°C for 18 s. Fluorescence was acquired at the end of every 72°C extension phase. In this assay, we employed a housekeeping gene, porphobilinogen deaminase (PBGD), as an internal standard [27]. The primers for *β3Gal-T1, T2, T3,* and *β3Gal-T4* were employed as described previously [20]. The specific primer for *β3Gal-T5* was designed to flank intronic sequences out of the DNA sequence (GenBank accession number AB020337; table 1).

Quantification data from each sample were analyzed using LightCycler analysis software [25]. In this analysis, the background fluorescence was removed by setting a noise band. The transcription value of the target was obtained by plotting on the standard curve. To construct standard curves for *β3Gal-T1, T2, T3, T4,* and *β3Gal-T5* and PBGD, cDNA was synthesized from total 1 μg RNA composed of CA 19-9-expressing cancer cells (SW1116) [28] and RNA isolated from *Escherichia coli.* Ten-fold serial dilution of SW1116, 10^{-1} to 10^{-4}, was adopted in the synthesis of cDNA. We have already confirmed that any PCR primer for this study could not amplify any product from *E. coli* [26]. The amount of each transcript was normalized according to that of PBGD quantified with the same sample. For distinguishing the specific product from nonspecific products and primer dimers, melting curves of final PCR products were analyzed [29]. Since different DNA products melt at different temperatures, it was possible to distinguish genuine products from primer dimers or nonspecific products [30].

Immunohistochemistry

Deparaffinized 4-μm-thick sections were treated with 0.3% hydrogen peroxide in absolute methanol for 20 min in order to block endogenous perodoxidase activity. The sections were then incubated with 1% bovine serum albumin in phosphate-buffered saline to block nonspecific antibody binding. Subsequently, slides were incubated with mouse monoclonal antihuman CA 19-9 antibody (clone 116-

Table 2. Clinical information on the patients with pancreatic tumors and expression of CA 19-9 and DUPAN-2 antigens

Patient No.	Sex	Age year	Histology	TMN classification	Stage	CA 19-9 value[1]	*Le* genotype	CA 19-9 grade[2]	DUPAN-2 grade[2]	*β3Gal-T5* expression[3]
1	F	64	mucinous	T2N0M0	III	22	*Le/Le*	3	3	23.8
2	M	66	mod. diff.	T2N0M0	III	606	*Le/le*	0	1	2.4
3	M	61	poorly diff.	T3N1M0	IVa	1,060	*Le/le*	2	3	2.7
4	F	66	mod. diff.	T3N0M0	IVa	<5	*le/le*	0	3	11.9
5	M	67	mod. diff.	T2N0M0	III	126	*Le/le*	1	0	1.5
6	M	72	well diff.	T2N2M0	IVa	<5	*Le/le*	3	2	9.2
7	F	79	mod. diff.	T3N1M0	IVa	89	*Le/le*	0	0	0.3
8	M	70	mod. diff.	T2N1M0	III	48	*Le/le*	1	1	2.6
9	M	72	well diff.	T3N1M0	IVa	56	*Le/Le*	3	3	10.5
10	F	57	well diff.	T1N1M0	II	70	*Le/Le*	0	1	1.5
11	F	64	mod. diff.	T3N1M0	IVa	546	*Le/le*	2	3	9.6
12	M	60	poorly diff.	T3N0M0	IVa	<5	*Le/Le*	2	2	6.7
13	F	45	mod. diff.	T3N3M0	IVb	378	*Le/Le*	2	3	5.3

mod. = Moderately; diff. = differentiated.
1 Normal range for serum CA 19-9 was below 37 U/ml.
2 Immunohistochemical grade.
3 *β3Gal-T5/PBGD.*

NS-19-9 IgG isotype; DAKO, Copenhagen, Denmark) at a final concentration of 2.5 μg/ml or with anti-DUPAN-2 antibody (IgM isotype; Kyowa Medex, Tokyo, Japan) at a final concentration of 5 μg/ml, overnight at 4°C. This was followed by incubation with biotinylated goat antimouse IgG or IgM (Vector Labs, Burlingame, Calif., USA) at a final concentration of 10 μg/ml, for 1 h at room temperature. Then, sections were allowed to react with an avidin-biotin system. Counterstaining was carried out with Mayer's hematoxylin.

All immunostained sections were coded and evaluated without prior knowledge of the clinical and pathological parameters. In each section, 5 high-power fields were selected at random, and a total number of at least 1,000 cells were evaluated. The results were expressed as the percentage of positively stained cells. The grade of staining was estimated on a scale from 0 to 3 (0 = stained less than 5% of the field; 1 = stained more than 5% but less than 25%; 2 = stained more than 25% but less than 50%, and 3 = stained more than 50%), as described previously [31]. All slides were estimated by 2 investigators who were blinded to the origin of the sections on 3 different occasions. When the results were different, the final diagnosis of these samples was determined with the investigators using a multihead microscope.

Statistical Analysis

Statistical analyses were performed using StatView™ version 5.0 (SAS Institute, Cary, N.C., USA) for Macintosh computers. Nonparametric (Mann Whitney) analysis was performed to ascertain statistical significance between the amount of each galactosyltransferase in noncancerous and cancerous tissues. A p value of less than 0.05 denoted the presence of statistically significant difference. Spearman's rank correlation test was done to determine the significance of the correlation coefficient for the relationship between each gene expression and immunohistochemical reactivities of CA 19-9 and DUPAN-2.

Results

Patients and Genotyping of the Le *Gene*

All tissues were diagnosed as having pancreatic carcinoma with various stages (1 with stage II, 4 with stage III, 7 with stage IVa and 1 with stage IVb). Of 13 pancreatic carcinomas, 1 was pathologically diagnosed as mucinous adenocarcinoma, and 3 were diagnosed as well, 7 as moderate and 2 as poorly differentiated adenocarcinoma. No significant correlation was observed between the serum level of CA 19-9 and age, gender, tumor differentiation or clinical stage (table 2).

Among the 13 patients, 1 patient had homozygote alleles of inactive *Le* gene alleles (*le/le*), which indicates that the patient genetically lacks the Le enzyme, as previously reported [32]. This *Le*-negative patient exhibited an undetectable amount of CA 19-9 in the serum. Five patients had the active *Le* gene homozygously *(Le/Le),* and the other 7 were determined to have the heterozygous *Le* genotype *(Le/le).* No difference in the serum values or immunoreactivity of CA 19-9 was observed between patients who were heterozygous for the *Le* allele and those